Conformation and Dynamics of the [3-^{13}C]Ala, [1-^{13}C]Val-Labeled Truncated *pharaonis* Transducer, *p*HtrII(1–159), as Revealed by Site-Directed ^{13}C Solid-State NMR: Changes Due to Association with Phoborhodopsin (Sensory Rhodopsin II)

Satoru Yamaguchi,* Kazumi Shimono,[†] Yuki Sudo,[†] Satoru Tuzi,* Akira Naito,[‡] Naoki Kamo,[†] and Hazime Saitô*

*Department of Life Science, Graduate School of Science, Himeji Institute of Technology, Harima Science Garden City, Kamigori, Hyogo, Japan; [†]Laboratory of Biophysical Chemistry, Graduate School of Pharmaceutical Sciences, Hokkaido University, Sapporo, Japan; and [‡]Graduate School of Engineering, Yokohama National University, Hodogaya-ku, Yokohama, Japan

ABSTRACT   We have recorded ^{13}C NMR spectra of the [3-^{13}C]Ala, [1-^{13}C]Val-labeled *pharaonis* transducer *p*HtrII(1–159) in the presence and absence of phoborhodopsin (*p*pR or sensory rhodopsin II) in egg phosphatidylcholine or dimyristoylphosphatidylcholine bilayers by means of site-directed (amino acid specific) solid-state NMR. Two kinds of ^{13}C NMR signals of [3-^{13}C]Ala-*p*HtrII complexed with *p*pR were clearly seen with dipolar decoupled magic angle spinning (DD-MAS) NMR. One of these resonances was at the peak position of the low-field α-helical peaks (α_{II}-helix) and is identified with cytoplasmic α-helices protruding from the bilayers; the other was the high-field α-helical peak (α_{I}-helix) and is identified with the transmembrane α-helices. The first peaks, however, were almost completely suppressed by cross-polarization magic angle spinning (CP-MAS) regardless of the presence or absence of *p*pR or by DD-MAS NMR in the absence of *p*pR. This is caused by an increased fluctuation frequency of the cytoplasmic α-helix from 10^5 Hz in the uncomplexed states to $>10^6$ Hz in the complexed states, leading to the appearance of peaks that were suppressed because of the interference of the fluctuation frequency with the frequency of proton decoupling (10^5 Hz), as viewed from the ^{13}C NMR spectra of [3-^{13}C]Ala-labeled *p*HtrII. Consistent with this view, the ^{13}C DD-MAS NMR signals of the cytoplasmic α-helices of the complexed [3-^{13}C]Ala-*p*HtrII in the dimyristoylphosphatidylcholine (DMPC) bilayer were partially suppressed at 0°C due to a decreased fluctuation frequency at the low temperature. In contrast, examination of the ^{13}C CP-MAS spectra of [1-^{13}C]Val-labeled complexed *p*HtrII showed that the ^{13}C NMR signals of the transmembrane α-helix were substantially suppressed. These spectral changes are again interpreted in terms of the increased fluctuation frequency of the transmembrane α-helices from 10^3 Hz of the uncomplexed states to 10^4 Hz of the complexed states. These findings substantiate the view that the transducers alone are in an aggregated or clustered state but the *p*pR-*p*HtrII complex is not aggregated. We show that ^{13}C NMR is a very useful tool for achieving a better understanding of membrane proteins which will serve to clarify the molecular mechanism of signal transduction in this system.

INTRODUCTION

Halobacteria express a family of four retinal proteins: bacteriorhodopsin (bR), halorhodopsin (hR), sensory rhodopsin I (sRI), and phoborhodopsin (pR or sensory rhodopsin II (sRII)). These proteins carry out two distinct functions through a common photochemical reaction (Spudich et al., 2000). The latter two sensory rhodopsins are photoreceptors involved in positive and negative phototaxis, respectively, and act through specific interactions with their cognate transducers (Hoff et al., 1997); bR and hR are light-driven ion pumps transporting, respectively, protons and chloride (Lanyi, 1999). *Pharaonis* phoborhodopsin (*p*pR) is a pigment protein from *Natronobacterium pharaonis* (Hirayama et al., 1992) which corresponds to pR of *Halobacterium salinarum* (Takahashi et al., 1985; Tomioka et al., 1986), with which it has 50% amino acid sequence homology (Seidel et al., 1995;

Kamo et al., 2001). However, its isolation from an over-expressing strain of *Escherichia coli* shows that it is more stable than pR (Shimono et al., 1997; Hohenfeld et al., 1999). These two photoreceptors, through their likely conformational changes, convey a light signal to a tight protein complex comprising the photoreceptor and its cognate transducer. The transducer has two transmembrane helices (Zhang et al., 1999) that modulate autophosphorylation, phosphorylating a bound cytoplasmic histidine kinase.

Three-dimensional structures of *p*pR along with its complex with the cognate truncated transducer *p*HtrII(1–114) have been recently determined by electron crystallographic analysis of two-dimensional crystals (Kunji et al., 2001) and by x-ray diffraction studies of three-dimensional crystals (Luecke et al., 2001; Royant et al., 2001; Gordeliy et al., 2002). *p*pR is highly similar to bR, although *p*pR has minor changes in the retinal pocket and has an unbent retinal, which reflects their respective biological functions of proton transport and signal transduction (Kunji et al., 2001; Luecke et al., 2001; Royant et al., 2001). In addition, transient movement of helix F in *p*pR and in receptor-transducer signal transfer were analyzed by means of electron paramagnetic resonance on spin-labeled *p*pR and *p*HtrII and their

complexes (Wegener et al., 2000, 2001). The movement of the F-helix and its interaction with *p*HtrII may explain the observation that *p*pR alone is able to perform photoinduced proton pumping, whereas its complex with *p*HtrII lacks this ability due to so-called cytoplasmic closure (Sudo et al., 2001a, 2002). The composition of the complex was predicted to be equal amounts of *p*pR and *p*HtrII (Sudo et al., 2001b) and this is consistent with the x-ray structure of the complex (Gordeliy et al., 2002) since the expected dimer of the complex is formed by a crystallographic twofold rotation axis located in the middle of four transmembrane helices and the transmembrane helices F and G of the receptor are in contact with the helices of the transducer. Nevertheless, it is still not clear how the activation of the transducer *p*HtrII by the receptor of *p*pR leads to a conformational change of the second transmembrane segment (TM2) that propagates to the tip of the coiled coil cytoplasmic domain. This domain comprises the linker, methylation, and signaling regions, similar to the highly conserved bacterial chemotaxis receptor (Gordeliy et al., 2002; Kim and Kim, 2002; Le Moual and Koshland, 1996). The structure of the linker region remains unsolved. In fact, the structure of TM2 ends with Leu-82, leaving residues 83–114 in multiple conformations as viewed from the recent x-ray diffraction study (Gordeliy et al., 2002).

We have demonstrated that the site-directed solid-state ^{13}C NMR approach is an excellent, nonperturbing means to delineate the conformation as well as the dynamics of membrane proteins at physiologically important ambient temperature once well-resolved ^{13}C signals are available from selectively ^{13}C-labeled proteins such as bR (Saitô et al., 1998, 2000, 2002a, 2004). We can assign signals to certain residues of interest, utilizing site-directed mutants and the conformation-dependent displacements of ^{13}C chemical shifts accumulated so far from appropriate model systems (Saitô, 1986; Saitô and Ando, 1989). Thus, this method has the potential to observe the conformation and dynamics of specific residues of membrane proteins. This approach turned out to be especially useful as a complement to diffraction studies where the structural data of rather flexible surfaces such as C- or N-terminals and loop regions are in many cases lost owing to a disordered or motionally averaged state (Saitô et al., 1998, 2000, 2002a,b). One example is that of [3-^{13}C] and [1-^{13}C]Ala-bR (Yamaguchi et al., 1998, 2000, 2001), where the C-terminal α-helix [226–235] protrudes from the cytoplasmic membrane surface where it plays an essential role in assembling the cytoplasmic surface structure (Yonebayashi et al., 2002). Recently, we have showed that a very similar spectral feature is seen in [3-^{13}C]Ala, [1-^{13}C]Val-labeled *p*pR, including the presence of the above-mentioned C-terminal α-helical segment. Further, we have shown that the dynamic features of *p*pR are significantly different when a complex is formed with the transducer *p*HtrII(1–159) (Arakawa et al., 2003).

In this article, we attempt to extend this approach to record ^{13}C NMR spectra of the [3-^{13}C]Ala, [1-^{13}C]Val-labeled cognate truncated transducer *p*HtrII(1–159) both in the free form and in a complex with *p*pR to gain insight into the conformation and dynamic features of the linker region (also called the HAMP domain) which might play a crucial role in the signal transduction of the sRI/HtrI system (Hoff et al. 1997) as well as in Tar and Tsr in pH sensing (Umemura et al., 2002). Since the full length of *p*HtrII cannot be expressed in *E. coli* cells (Sudo et al., unpublished data), we used a truncated transducer *p*HtrII(1–159) which has advantage in that we are able to observe more signals from the linker region than in the full-length version. Samples are reconstituted in an egg phosphatidylcholine (PC) or in a dimyristoylphosphatidylcholine (DMPC) bilayer. We find the presence of an α-helical segment with a possible coiled coil form in this region as viewed from ^{13}C chemical shifts of [3-^{13}C]Ala residue with reference to the conformation-dependent displacements (Saitô et al., 2000, 2002a).

MATERIALS AND METHODS

[3-^{13}C]Ala, [1-^{13}C]Val-labeled truncated C-terminal-histidine (6 × His)-tagged *pharaonis* halobacterial transducer *p*HtrII(1–159) was expressed in *E. coli* BL21 (DE3) cultured in the M9 medium to which ^{13}C-labeled L-Ala and L-Val were added. The protein was solubilized with 1.5% *n*-dodecyl β-D-maltoside (DM), followed by purification with Ni-NTA resin (Qiagen) as described previously (Sudo et al., 2001b). Here *p*HtrII(1–159) is *p*HtrII expressed from the first to the 159th position, and Ala and Val residues in this region are circled and boxed in Fig. 1 (based on Seidel et al., 1995). *p*pR with a 6 × His-tag at the C-terminus was expressed in *E. coli* BL21 (DE3) cultured in M9 medium and purified as reported (Kandori et al., 2001). The purified protein in a DM solution was mixed with a lipid film of egg PC or DMPC (1:50 mol ratio) formed on the inner surface of the flask, followed by gentle stirring on ice overnight. DM was removed with Bio-Beads (SM22,
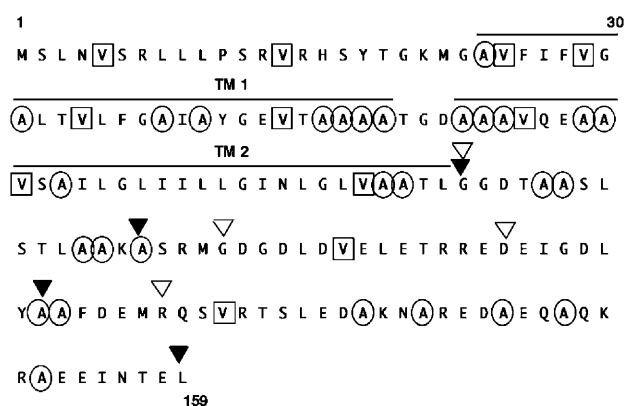

FIGURE 1 Amino acid sequence of truncated *pharaonis* *p*HtrII(1–159) (Seidel et al., 1995). Two transmembrane α-helices, TM1 and TM2, are shown by the bars above the sequence. Location of ^{13}C-labeled Ala and Val residues are indicated by the circles and boxes, respectively. The beginnings and ends of plausible coiled coil forms are shown by the two solid triangles above the amino acid residues under consideration. The predicted coiled coil form by Le Moual and Koshland (1996) are also shown as portions between the two open triangles.

BioRad, Hercules, CA) to yield *p*HtrII incorporated into the egg PC bilayer. The reconstituted preparation was further concentrated by centrifugation and suspended in 5 mM HEPES (pH 7) buffer containing 10 mM NaCl. The *p*pR/*p*HtrII(1–159) complex reconstituted in phospholipids was prepared as follows: the 1:1 mixture of *p*HtrII(1–159) with *p*pR in DM was mixed with a lipid film as described above and dialyzed to remove DM using Bio-Beads. The stoichiometry of the complex is found to be at least 1:1 as viewed from Fourier transform infrared spectroscopy (Furutani et al., 2003) but is more likely to be 2:2 (Wegener et al., 2001; Yang and Spudich, 2001). Just before solid-state NMR measurements, samples were dialyzed against pure water. Pelleted preparations of uncomplexed *p*HtrII(1–159) or its complex with ppR were placed in a 5-mm o.d. zirconia pencil-type rotor for magic angle spinning after being rapidly and tightly sealed with Araldite (Vantico, East Lansing, MI) to prevent leakage or evaporation of water from the samples during magic angle spinning under a stream of dried compressed air.

High-resolution solid-state ^{13}C NMR spectra of fully hydrated preparations were recorded on a Varian (Palo Alto, CA) CMX 400 Infinity NMR spectrometer ([13]C:100.6 MHz) at temperatures (30°–0°C) by cross-polarization magic angle spinning (CP-MAS) and single-pulse, dipolar decoupled magic angle spinning (DD-MAS). The latter approach turned out to be especially useful to distinguish ^{13}C NMR signals of flexible portions—such as N- or C-terminus and cytoplasmic α-helices protruding from the membrane surface—of fully hydrated [3-^{13}C]Ala-labeled membrane proteins from those rigid segments such as transmembrane α-helices and loops, because ^{13}C NMR signals in the former are usually suppressed in the presence of rapid molecular motion with fluctuation frequency $>10^6$ Hz owing to reduced cross-polarization rate. Furthermore, fluctuation frequencies in the order of 10^5 or 10^4 Hz arising from such cytoplasmic and transmembrane α-helices were readily evaluated by careful examination of suppressed or recovered peak intensities of ^{13}C NMR signals from [3-^{13}C]Ala and [1-^{13}C]Val-labeled proteins, respectively. This is because the corresponding ^{13}C NMR signals of particular residues were preferentially suppressed when the incoherent fluctuation frequency of such residues

might interfere with the coherent frequency of either proton decoupling (10^5 Hz for [3-^{13}C]Ala-labeled portion) or magic angle spinning (10^4 Hz for [1-^{13}C]Val-labeled portion) (Suwelack et al., 1980; Rothwell and Waugh, 1981; Saitô et al., 2000, 2002a). Spectral width, acquisition, and contact times for the CP-MAS measurements were 40 kHz, 50 ms, and 1 ms, respectively. A proton decoupling frequency of 50 kHz was used. The $\pi/2$ pulses for both carbon and proton nuclei were 5.0 μs and the spinning rate was 4 kHz. Repetition times for the CP-MAS and DD-MAS spectra were 4.0 and 6.0 s, respectively, and a $\pi/4$ pulse for ^{13}C nuclei was used for the latter. Free induction decays were acquired with 2 K data points and accumulated 5000–20,000 times. Fourier transform was performed with 16 K points after 14 K points were zero-filled. [13]C chemical shifts were compared to tetramethylsilane through the carboxyl ^{13}C chemical shift of glycine (176.03 ppm).

RESULTS

Fig. 2 illustrates the ^{13}C DD-MAS (*left*) and CP-MAS (*right*) NMR spectra of [3-^{13}C]Ala-labeled *p*HtrII(1–159), where Fig. 2, *A* and *B*, are from the complex with *p*pR, and Fig. 2, *C* and *D*, are from uncomplexed *p*HtrII. Spectra were recorded at ambient temperature from the samples reconstituted in an egg PC bilayer. All the Ala C_β ^{13}C NMR signals from the protein (15.0–16.9 ppm) recorded by DD-MAS NMR can be assigned to the peak position of the α_{II}-helix (16.9–15.5 ppm) and its boundary with the ordinary α_I-helix (15.5–15.0 ppm), with reference, respectively, to the ^{13}C chemical shifts of (Ala)$_n$ in hexafluoroisopropanol (HFIP) solution or solid state (Krimm and Dwivedi, 1982; Tuzi et al., 1994; Kimura
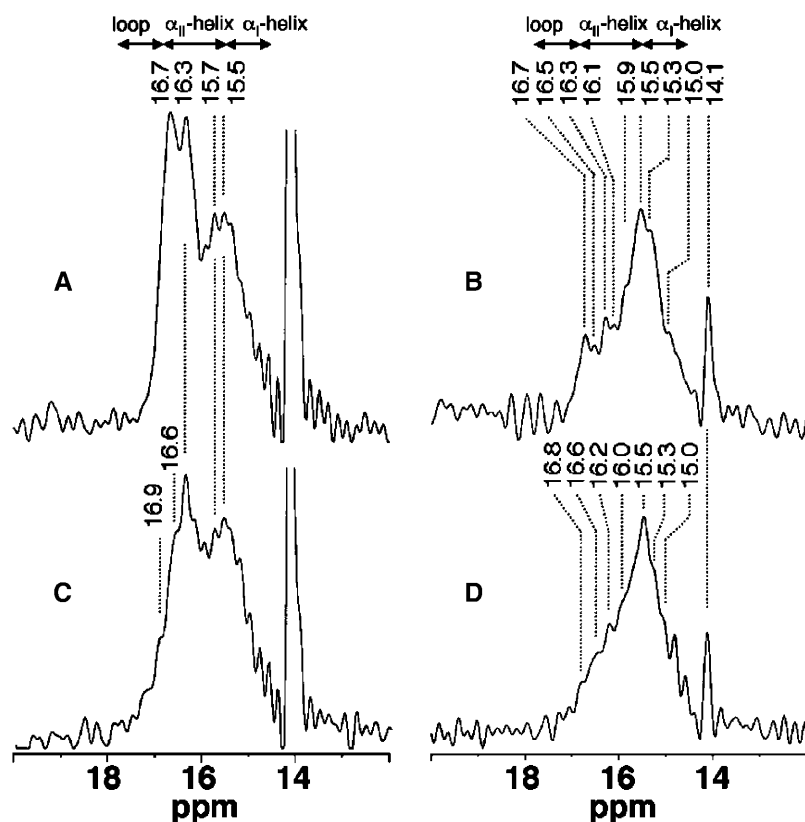

FIGURE 2 ^{13}C DD-MAS (*left*) and CP-MAS (*right*) NMR spectra of [3-^{13}C]Ala-labeled *pharaonis* truncated *p*HtrII(1–159) in complex with *p*pR (*A* and *B*), reconstituted in egg PC bilayer, as compared with those in the absence of *p*pR (*C* and *D*). ^{13}C NMR signals of high-field region (12–20 ppm) from the [3-^{13}C]Ala-proteins alone are presented. The intense or sharp ^{13}C NMR signal resonated at the highest peak position 14.1 ppm is ascribed to methyl peak of egg PC.

et al., 2001; Saitô et al., 2002a); this is the case because no ^{13}C NMR signal appears at the position of the random coil (16.9 ppm) or β-structure (19.9 ppm) (Saitô, 1986; Saitô and Ando, 1989; Tuzi et al., 1994; Saitô et al., 2000, 2002a). In addition, the intense ^{13}C NMR peak at 14.1 ppm can be assigned to that of the methyl group from egg PC.

The intense α_{II}-helical ^{13}C NMR peaks resonated at 16.7 and 16.3 ppm as a doublet peak for pHtrII(1–159) complexed with ppR, with an additional broad envelope at 15.5 ppm, as recorded by the DD-MAS NMR (Fig. 2 A). Such low-field intense α_{II}-helical peaks, however, were obviously suppressed when the ^{13}C NMR spectra were recorded by CP-MAS NMR (Fig. 2 B), leaving the signals of the high-field envelope peaks at 15.5 ppm unchanged. This is the case where the peaks under consideration were preferentially suppressed by a reduced cross-polarization rate owing to the presence of rapid molecular motion (with correlation time or fluctuation frequency in the order of $<10^{-6}$ s or $>10^6$ Hz, respectively). This finding is consistent with previous observations about the C-terminal α-helix protruding from the surface of bR (Saitô et al., 2000, 2002b; Yamaguchi et al., 2001; Yonebayashi et al., 2002) and ppR (Arakawa et al., 2003). The relative proportion of the low-field doublet, which is suppressed by CP-MAS NMR, to the high-field envelope peaks, including contributions from the unsuppressed peaks extending to the peak position of the α_{II}-helix in this DD-MAS NMR experiment, is found to be 38%:62% as judged from the relative peak intensities recorded by the ^{13}C DD-MAS and CP-MAS spectra, respectively (Fig. 2, A and B); this is very close to the relative proportion of Ala residues involved in the C-terminal cytoplasmic α-helix as compared to those of the transmembrane α-helices, 43%:57%. Therefore, the low-field α_{II}-helix and high-field

envelope peaks are unambiguously assigned, respectively, to the cytoplasmic and transmembrane α-helices.

Surprisingly, it appears that the low-field doublet peaks of the ^{13}C NMR signals of [3-^{13}C]Ala-pHtrII(1–159) in the absence of ppR are not always fully visible at ambient temperature, because they are substantially suppressed even by the DD-MAS (Fig. 2 C). The resulting dynamics change leads to a failure in our attempt to fully detect ^{13}C NMR signals by narrowing the peaks in the free state, due to interference of the incoherent frequency of motional fluctuations with the coherent frequency of proton decoupling essential for the successful peak narrowing (Rothwell and Waugh, 1981). The lowered fluctuation frequencies in the cytoplasmic α-helix of pHtrII(1–159) from $>10^6$ Hz of the complexed to the order of 10^5 Hz (5×10^4 Hz) of the free states, resulted in the preferentially suppressed peak intensities at 16.7 and 16.3 ppm, as a result of interference of fluctuation frequency with proton-decoupling frequency, as viewed from the ^{13}C NMR signals of [3-^{13}C]Ala-labeled residues (summarized in Table 1). It appears, however, that this observation conflicts with our expectation: fluctuation motions of the cytoplasmic α-helices of the transducer alone should be more pronounced in the free state than in the complexed state, because the frequency of the local fluctuation motions in the free state also depends upon the resulting reduced "effective molecular mass" and interhelical interactions. In fact, this view is confirmed when one compares the fluctuation frequencies of the transmembrane α-helices of ppR as estimated from the ^{13}C NMR spectra of [1-^{13}C]Val-ppR with and without pHtrII as summarized also in Table 1 (Arakawa et al., 2003), although the corresponding spectral changes are rather less pronounced as compared with those of the present observation for [1-^{13}C]Val-

TABLE 1 Fluctuation frequencies of free and complexed pHtrII(1–159) with ppR based on the manner of suppressed peak intensities in egg PC bilayer at 20°C

| | Free | | | | Complexed | | | | | |
| | Fluctuation frequency (Hz)* | Based on | [3-^{13}C]Ala | | [1-^{13}C]Val | Fluctuation frequency (Hz)* | Based on | [3-^{13}C]Ala | | [1-^{13}C]Val | |
Protein			CP-MAS	DD-MAS	CP-MAS			CP-MAS	DD-MAS	CP-MAS	Reference
pHtrII											
Cytoplasmic α-helices	$10^{5\dagger}$	Ala	S	PS	—‡	$>10^6$	Ala	S	NS	—‡	This article
Transmembrane α-helices	$10^{3\S}$	Val	NS	NS	PS	$10^{4\P}$	Val	NS	NS	S	This article
ppR											
Transmembrane α-helices	10^4–10^5	Val			NS	10^4	Val			PS	Arakawa et al. (2003)

Definitions of abbreviations in this table are as follows: S, suppressed; PS, partially suppressed; NS, not suppressed.
*Estimated order; these fluctuation frequencies of 10^4 and 10^5 Hz correspond to 4×10^3 Hz and 5×10^4 Hz, respectively. These values also correspond to the correlation times of 2.5×10^{-4} and 2×10^{-5} s, respectively.
†Frequency estimated by interference with the proton decoupling frequency.
‡No Val residue as a probe for this region.
§Frequency estimated by recovered from suppressed peaks due to interference with frequency of magic angle spinning.
¶Frequency estimated by interference with frequency of magic angle spinning.

*p*HtrII(1–159). This obvious conflict, however, may be compromised only when the uncomplexed transducers are not present as a monomer or dimer but exist as aggregated or clustered forms in the lipid bilayer. This finding also rules out the possibility that this moiety is a random coil even in the absence of *p*pR. Otherwise, it would be expected that the intensity of the ^{13}C NMR signal from the random coil would resonate at the characteristic peak position of 16.9 ppm, and should be invariant in spite of the presence or absence of *p*pR.

We attempted similar experiments by examining the ^{13}C NMR spectra of [3-^{13}C]Ala-pHtrII(1–159) complexed with *p*pR as reconstituted in a DMPC bilayer (Fig. 3) to examine how the previously noted spectral change is influenced by the flexibility of surrounding lipids at 20° and 0°C. As pointed out, the lipid phase of saturated fatty acyl chains can be very conveniently monitored by examination of the ^{13}C chemical shift of the methylene group of fatty acyl chains either in the gel (*trans* form of methylene chain; 32.6 ppm) or liquid crystalline phase (*gauche/trans* form of methylene chain; 30.3 ppm) (Kimura et al., 2001; Saitô et al., 2003). The ^{13}C chemical shifts of methylene peaks of the fatty acyl moieties of the DMPC bilayer were found to be 32.28 (with a half-bandwidth of 170 Hz) and 32.65 ppm (with a half-bandwidth of 110 Hz) at 20° and 0°C, respectively (spectra not shown). Obviously, the lipid phase of the DMPC bilayer at 20°C turned out to be at an intermediate stage of a broadened gel to liquid crystalline transition due to the presence of proteins in which both lipid conformations are present and which undergo fast conformational change. In fact, the broadened NMR peaks of the fatty acyl chains with a half-band width (170 Hz) are consistent with this view. As a result, the relative ^{13}C peak-intensity of the low-field cytoplasmic α-helical peaks in the DD-MAS NMR spectra in a DMPC bilayer (Fig. 3 *A*) is substantially reduced in the lipids of intermediate gel phase as compared with those of liquid crystalline egg PC bilayer (Fig. 2 *A*).

Fig. 4 summarizes how the ^{13}C DD-MAS NMR spectra of [3-^{13}C]Ala-pHtrII(1–159) complexed with *p*pR reconstituted in egg PC bilayer varied with temperature. It appears that there are two kinds of spectral changes at both the cytoplasmic and transmembrane α-helices as can be seen by raising or lowering the temperature. The relative peak intensity of the envelope peak resonated at the boundary between the $α_I$- and $α_{II}$-helical peaks of the transmembrane α-helices at 15.5 ppm seemed to be gradually suppressed when the temperature was raised from 20° to 30°C, probably due to the onset of partial suppression caused by the interference of fluctuation frequencies with the proton decoupling frequency (Rothwell and Waugh, 1981). In contrast, the peak intensities of the low-field cytoplasmic α-helices at 16.7 and 16.3 ppm are substantially decreased at temperatures <10°C. This is obviously caused by the suppression of the peaks due to lowered fluctuation frequency of the C-terminal α-helix from $\sim$>10^6 Hz at ambient temperature to $\sim$$10^5$ Hz at low temperature, which interferes with the proton decoupling frequency.

Fig. 5 demonstrates the ^{13}C DD-MAS (*left*) and CP-MAS (*right*) NMR spectra of [1-^{13}C]Val-labeled *p*HtrII(1–159) reconstituted in an egg PC bilayer at ambient temperature: the upper two panels refer to a *p*pR complex (Fig. 5, *A* and *B*) and the lower two (Fig. 5, *C* and *D*) to free *p*pR. It is striking
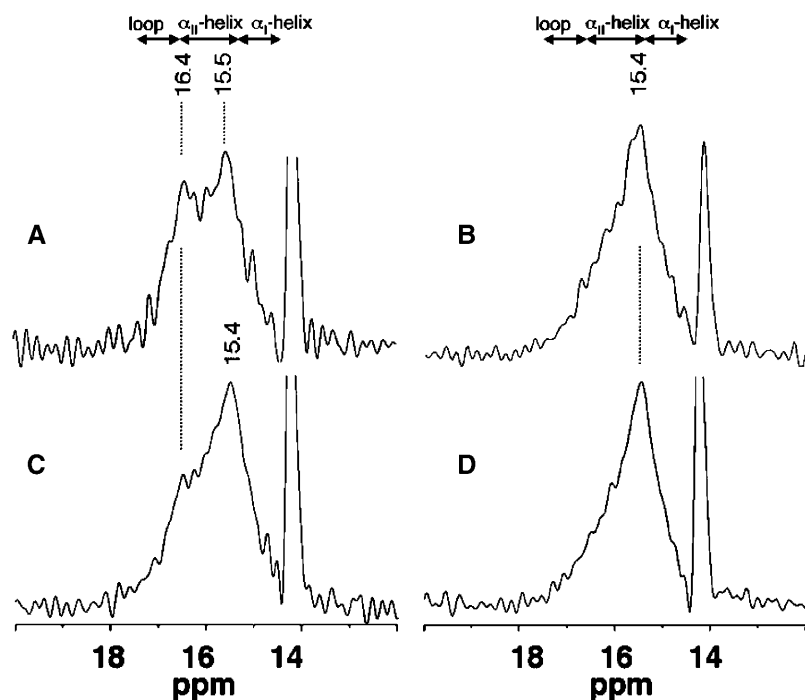

FIGURE 3 ^{13}C DD-MAS (*left*) and CP-MAS (*right*) NMR spectra of [3-^{13}C]Ala-labeled *p*HtrII(1–159) reconstituted in DMPC bilayer, recorded at 20°C (*A* and *B*) and 0°C (*C* and *D*), respectively.
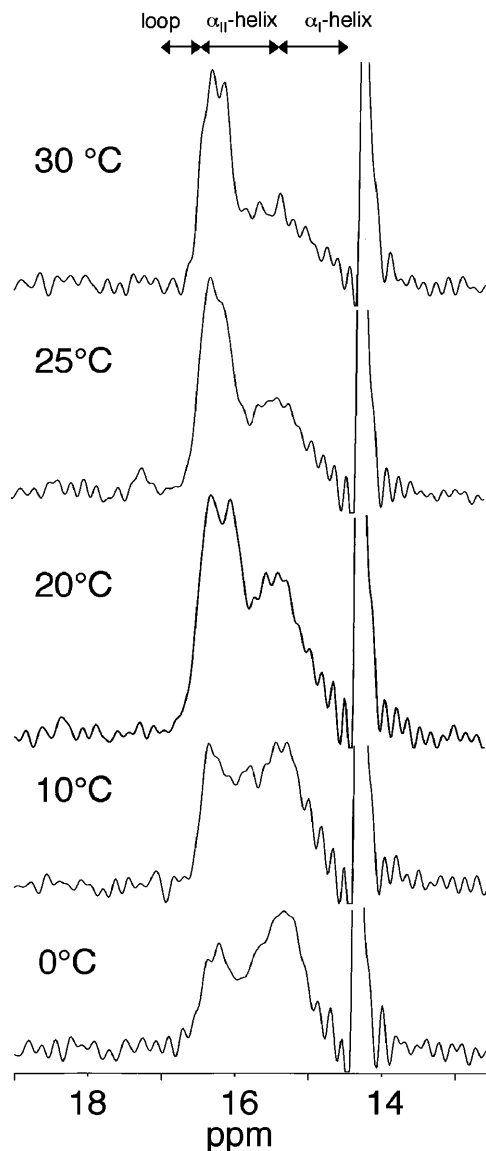
FIGURE 4 ^{13}C DD-MAS NMR spectra of [3-^{13}C]Ala-labeled *pharaonis* truncated *p*HtrII(1–159) complexed with *p*pR, reconstituted in egg PC bilayer, recorded at various temperatures.

from the CP-MAS NMR spectral data that very weak and broad featureless ^{13}C NMR signals are observed from the transmembrane α-helices of [1-^{13}C]Val-*p*HtrII (1–159) complexed with *p*pR in the egg PC bilayer (Fig. 5 *B*), whereas more intense ^{13}C NMR signals at 174.3–177 ppm are observed from those portions in the absence of *p*pR (Fig. 5 *D*) and are assigned to Val residues involved in the transmembrane α-helices. It also appears that two Val residues are involved in the cytoplasmic α-helices of *p*HtrII(1–159) (see Fig. 1). Therefore the fluctuation frequencies of the transmembrane α-helices as viewed from the ^{13}C NMR signals of [1-^{13}C]Val-labeled residues were estimated as the order of 10^3 and 10^4 Hz (4×10^3 Hz or 2.5×10^{-4} s as fluctuation frequency or correlation time, respectively) for

the free and complexed transducer on the basis of frequencies corresponding to the recovered and suppressed peaks, respectively, as summarized in Table 1. An alternative possible frequency of 10^5 Hz for the former is readily ruled out, because the ^{13}C NMR signals from [3-^{13}C]Ala-*p*HtrII(1–159) was not suppressed. We also note that there appears to be no contribution of a β-structure, as in the above-mentioned model system (Saitô, 1986; Saitô et al., 2000, 2002a). This is in contrast to that of the ^{13}C NMR spectra changes of the complexed and free [3-^{13}C]Ala-*p*HtrII(1–159) as illustrated in Fig. 2, *A* and *B*, as well as Fig. 2, *C* and *D*, although for the latter this is true to a lesser extent. The intense sharp ^{13}C signal at 173.6 ppm is most pronounced in the DD-MAS NMR spectra (Saitô et al., 2003; Fig. 5, *A* and *C*), because the previously seen ^{13}C NMR signals from the transmembrane α-helices were not efficiently observed due to a longer spin-lattice relaxation time as compared with the repetition time. Accordingly, the 173.6 ppm signal with shorter spin-lattice relaxation time is readily assigned to the carbonyl carbons from the egg PC bilayer (Arakawa et al., 2003; Saitô et al., 2003). Here it should be taken into account that there are two Val residues in both the N- and C-terminus. Accordingly, the ^{13}C NMR signal from the two [1-^{13}C]Val-residues in the N-terminus that are probably in a random-coil form (Saitô et al., 2004) might be accidentally superimposed upon this carbonyl carbon signal of the egg PC bilayer.

DISCUSSION

Conformational characterization of *p*HtrII with emphasis on its cytoplasmic domain

As previously pointed out in our previous work on the conformation-dependent displacement of peaks (Saitô, 1986; Saitô and Ando, 1989; Saitô et al., 2002a, 2004), conformational characterization of *p*HtrII(1–159) is feasible in the presence or absence of *p*pR, as viewed from the ^{13}C chemical shifts of [3-^{13}C]Ala and [1-^{13}C]Val-labeled preparations. It is important to note that the two types of ^{13}C NMR peaks of free and complexed [3-^{13}C]Ala-*p*HtrII(1–159) are unambiguously assigned to the cytoplasmic and transmembrane α-helices, as described already (see Figs. 2–4) (Tuzi et al., 1994; Saitô et al., 2002a,b; Arakawa et al., 2003). We demonstrate here that the ^{13}C NMR signals of [3-^{13}C]Ala-labeled *p*HtrII(1–159) complexed with *p*pR are fully visible (Fig. 2 *A*) but that the low-field ^{13}C NMR signal of the cytoplasmic α-helix was partially suppressed in the absence of *p*pR as recorded by the DD-MAS method (Fig. 2 *C*). In contrast, rather intense ^{13}C NMR signals were recorded for the uncomplexed [1-^{13}C]Val-labeled *p*HtrII(1–159) (Fig. 5 *D*), whereas ^{13}C NMR signals of [1-^{13}C]Val-*p*HtrII complexed with *p*pR were completely suppressed by CP-MAS (Fig. 5 *C*). It should be taken into account that this distinction is based on a one-order magnitude difference in
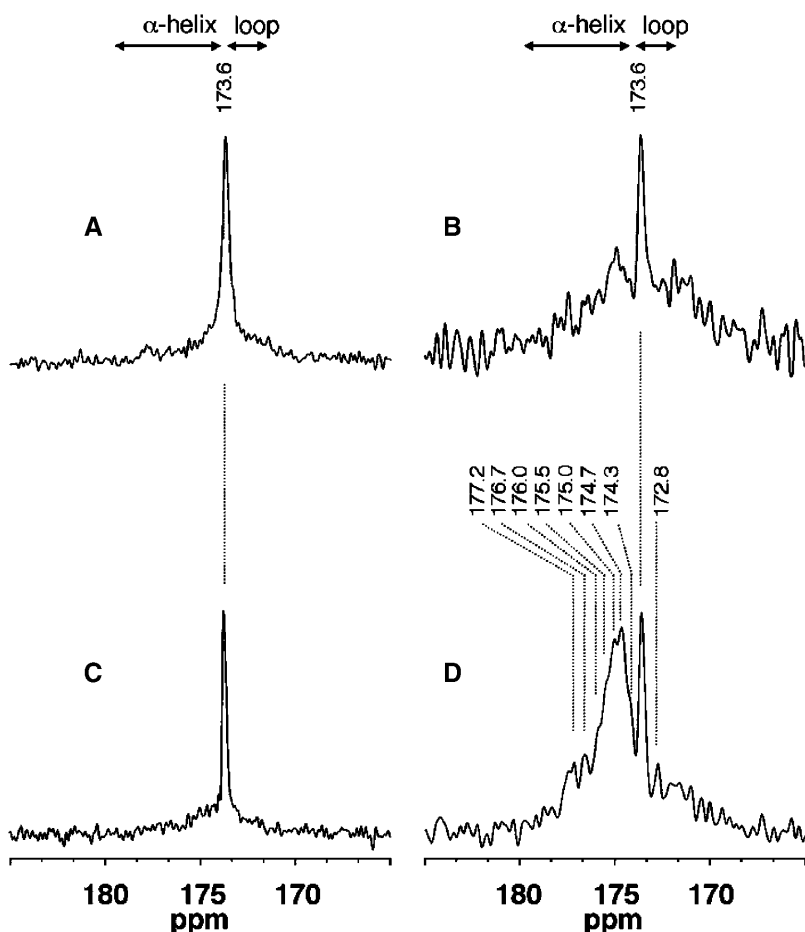
FIGURE 5 ^{13}C DD-MAS (*left*) and CP-MAS (*right*) NMR spectra of [1-^{13}C]Val-labeled *pharaonis* truncated *p*HtrII(1–159) in complex with *p*pR (*A* and *B*), reconstituted in egg PC bilayer, as compared with those in the absence of *p*pR (*C* and *D*). The peak at 173.6 ppm arose from the carbonyl peak of egg PC.

the fluctuation frequencies interfered with a frequency of proton decoupling (10^5 Hz (or 5×10^4 Hz) for signals of [3-^{13}C]Ala-protein) or magic angle spinning (10^4 Hz (or 4×10^3 Hz) for the [1-^{13}C]Val-labeled protein). The relative proportion of the peak intensities of the former to the latter is consistent with the relative amount of Ala residues distributed in the respective regions (Fig. 2 *A*), as previously stated. On the contrary, the ^{13}C NMR signals from [1-^{13}C]Val-*p*HtrII(1–159) are mainly due to the transmembrane α-helices recorded by CP-MAS NMR, although ^{13}C signals from the two Val residues in the N-terminal domain might be superimposed upon the peak position of egg PC at 173.6 ppm as a random coil as recorded by the DD-MAS NMR spectra (Fig. 5, *A* and *C*). We emphasize that there appears to be no ^{13}C NMR signal from Ala residues involved in a loop or random coil form, as judged from their ^{13}C chemical shift data. Naturally, this finding is consistent with the previous data based on x-ray diffraction showing that Ala residues are not involved in the cytoplasmic loops (see Fig. 1). The absence of the ^{13}C NMR peak from the random coil portion in the C-terminus of [3-^{13}C]Ala-*p*HtrII, however, is in contrast to our previous observations for [3-^{13}C]Ala-labeled bR (Saitô et al., 2000) and *p*pR (Arakawa et al.,

2003). This means that all the Ala residues located at the cytoplasmic domain of *p*HtrII(1–159) are involved in an ordered conformation such as an α_{II}-helix form.

The presence of the α_{II}-helix instead of an ordinary α-helix (α_I-helix) for bR was initially proposed by Krimm and Dwivedi (1982) on the basis of infrared spectral data: the majority of the transmembrane α-helices in bR are not in the standard α-helix form in which the amide planes are all nearly parallel to the helical axis. Instead, they propose, from Fourier transform infrared spectroscopy measurements of bR—as compared to (Ala)$_n$ in HFIP solution—that they are in an α_{II}-helix in which the amide plane becomes significantly tilted with respect to the helical axis. Nevertheless, this was not observed from the three-dimensional structure of cryoelectron microscopy or from x-ray diffraction studies at low temperature (Grigorieff et al., 1996; Luecke et al., 1999). Instead, the ^{13}C NMR peak, which is significantly displaced downfield from the peak position of the α_I-helix, defines the α_{II}-helix from the NMR point of view, with reference to the ^{13}C chemical shift of (Ala)$_n$ in HFIP solution based on the definition of Krimm and Dwivedi (1982). However, no significant spectral change appears in the NMR data of bR labeled with [1-^{13}C]Ala, Val, etc. (Saitô

et al., 2000, 2002a). Instead of the initial proposal by Krimm and Dwivedi (1982), therefore, it seems more reasonable to consider that the so-called α_{II}-helix of [3-^{13}C]Ala-labeled proteins, defined with reference to the ^{13}C chemical shift of (Ala)$_n$ in HFIP solution, should be ascribed to a residue whose time-averaged torsion angles for the α-helix at ambient temperature are not always the same as those of the static one achieved at low temperature because of the presence of low-frequency local anisotropic fluctuation (Kimura et al., 2001). We emphasize here that the presence of such low frequency motions, if any, might also result in specific peak suppression for [3-^{13}C]Ala residues located at the transmembrane helices near the surface, depending upon the exact frequency that interferes with the proton decoupling frequency (Kawase et al., 2000; Saitô et al., 2000, 2002a; Yamaguchi et al., 2000). Interestingly, the ^{13}C NMR signals of [3-^{13}C]Ala-labeled residues of pHtrII(1–159) located at the cytoplasmic domain are ascribed to the cytoplasmic α-helix as present at the peak position of the α_{II}-helix, as will be discussed later. These peaks, however, were substantially suppressed when the spectra were recorded by CP-MAS NMR because of the reduced efficiency of cross-polarization arising from rapid fluctuation motions. In any case, the present ^{13}C NMR observations provide direct evidence for the presence of the α-helix conformation in the cytoplasmic domain of pHtrII(1–159).

The predicted secondary structure of the cytoplasmic domain as calculated by the method of Chou and Fasman (1978) turned out to be mainly α-helical between Ser-81 and Arg-99 and between Gly-103 and Glu-158, with interruption of the α-helix between Met-100 and Asp-102. Interestingly, our present finding based on the conformation-dependent displacement of ^{13}C chemical shifts (Saitô, 1986; Saitô and Ando, 1989; Saitô et al., 2002a, 2004) is consistent with the Chou-Fasman prediction, as viewed from the ^{13}C chemical shifts of Ala residues as intrinsic probes. Naturally, such an ordinary single helical portion protruding from the membrane surface extending from Gly-83, and participating in a plausible three-turn helix, might be in close contact with the C-terminal α-helix from ppR in view of the recently published x-ray structure (Gordeliy et al., 2002).

Instead, a coiled coil form may be formed at the C-terminal residues in the above-mentioned α_{II}-helical peaks to make the helix more rigid than the isolated single-stranded α-helix. In fact, a wide range of structural proteins have coiled coils in which two or three α-helices are wound around each other to form a left-handed superhelix conformation (Crick, 1953). The presence of this structure in a protein is apparent from the amino acid sequence alone because of the regularity of the α-helix structure which repeats every seven residues, the so-called heptad repeat; the apolar stripe between helices is defined by hydrophobic side chains at residues a and d in the sequence a-b-c-d-e-f-g, whereas electrostatic interactions occur between residues e and g. In view of the amino acid sequence in Fig. 1, such

a heptad repeat obviously occurs in the cytoplasmic domain, both at the initial portion between Gly-83 and Ala-97 and also between Ala-122 and beyond, as marked by the four closed triangles above the amino acid residues. The predicted coiled coil structures of α5 and α6 helices proposed by Le Moual and Koshland (1996) are also shown as portions between the open triangles above the sequence. As mentioned above, it is probable that the latter portion may participate in such supercoiling.

Dynamics-dependent ^{13}C NMR spectral features of membrane proteins

It should be borne in mind that ^{13}C NMR signals of even fibrous proteins such as collagen fibrils (Saitô and Yokoi, 1992) or crystalline peptide (Kamihira et al., 1998) are not always fully visible at ambient temperature by CP-MAS and DD-MAS NMR spectra, unless they are completely static, and free from any kind of backbone and side-chain motions. This is especially true for fully hydrated membrane proteins, because their ^{13}C NMR spectra recorded at ambient temperature might be suppressed due to the presence of possible internal fluctuations to be interfered with frequency of proton decoupling or magic angle spinning (Suwelack et al., 1980; Rothwell and Waugh, 1981; Saitô et al., 2000, 2002a). In particular, we showed here that the ^{13}C NMR peaks of the low-field cytoplasmic α-helices from the uncomplexed [3-^{13}C]Ala-pHtrII(1–159) are substantially suppressed (Fig. 2 C) as compared with those of the 2:2 complex with ppR (Furutani et al., 2003; Wegener et al., 2001; Yang and Spudich, 2001) (Fig. 2 A).

The estimated fluctuation frequencies for the cytoplasmic and transmembrane α-helices in the complexed state turned out to be in the order of $>10^6$ and 10^4 Hz, respectively, as judged by the recovered and suppressed peaks from the ^{13}C NMR peaks of [3-^{13}C]Ala- and [1-^{13}C]Val-pHtrII(1–159), respectively, complexed with ppR, although the corresponding fluctuation frequencies in the free state turned out to be 10^5 and 10^3 Hz (Table 1). As previously stated, the fluctuation frequency (10^4 Hz) of the transmembrane α-helices of pHtrII complexed with ppR is consistent with our former data from [3-^{13}C]Ala, [1-^{13}C]Val-labeled ppR complexed with pHtrII (Arakawa et al., 2003). We also showed that the fluctuation frequency of the latter was decreased one order of magnitude from 10^4–10^5 Hz in the free state to 10^4 Hz in the complex when the complex was formed as shown in Table 1, consistent with our expectation based on the increased ''molecular mass'' and tight helix-helix interactions as the result of complex formation due to specific protein-protein interaction as mentioned above. In reference to the fluctuation frequencies summarized in Table 1, the following two points should be taken into account. First, the fluctuation frequencies of the cytoplasmic α-helices are at least two orders of magnitude higher than those of the transmembrane α-helices in both the free and the complexed

states. This observation is consistent with expectation, because CH_3 groups of Ala residues in the former are able to acquire additional flexibility owing to their locations protruding from the membrane surface, together with the presence of a threefold rotation. Second, the fluctuation frequencies in the free state of *p*HtrII ($\sim 10^3$ Hz) increased one order of magnitude when it formed the complex with *p*pR. In addition, this fluctuation frequency of the free state is much smaller than that of monomeric bR ($\sim 10^4$ Hz) (Saitô et al., 2002b, 2003) and of bR fragment A(6–32) ($\sim 10^5$ Hz) (Kimura et al., 2001). Note that such fluctuation frequency is roughly inversely proportional to its ''effective'' molecular mass and its value for bR in two-dimensional crystal is $\sim 10^2$ Hz (Saitô et al., 2002a). This finding suggests that effective molecular mass of the transducer in lipid bilayer is much larger than that of monomeric bR or its fragment. The interpretation of this observation is unknown at present and is awaited for a further investigation. One possibility, however, is that *p*HtrII alone (in the free state) is not present as a monomer but as an aggregated or clustered state, and that the (2:2)-complex formed in the presence of *p*pR is neither aggregated nor clustered. The aggregated state of *p*HtrII alone in bilayer membrane is in parallel with a previously proposed view that homologous bacterial chemotaxis receptors from *E. coli* are aggregated to form clustered patches both in vivo and in vitro (Kim and Kim, 2002; Lybarger and Maddock, 2000; Levit et al., 2002).

In conclusion, we have pointed out that the present ^{13}C solid-state NMR approach is a very useful means to delineate a conformational feature of the transducer both in the cytoplasmic and transmembrane α-helices, based on the conformation-dependent displacements of ^{13}C chemical shifts. In addition, it is emphasized that a clear distinction is made as to whether a unique 1:1 or 2:2 complex, which is essential for the signal transduction, is formed between *p*pR and the *p*HtrII, as manifested from the changes in the backbone dynamics of their respective components on the basis of the suppressed or recovered peak intensities in the ^{13}C NMR.

REFERENCES

Arakawa, T., K. Shimono, S. Yamaguchi, S. Tuzi, Y. Sudo, N. Kamo, and H. Saitô. 2003. Dynamic structure of *pharaonis* phoborhodopsin (sensory rhodopsin II) and complex with a cognate truncated transducer as revealed by site-directed ^{13}C solid-state NMR. *FEBS Lett.* 536: 237–240.

Chou, P. Y., and G. D. Fasman. 1978. Empirical predictions of protein conformation. *Annu. Rev. Biochem.* 47:251–276.

Crick, F. H. C. 1953. The packing of α-helices: simple coiled coils. *Acta Crystallogr.* 6:689–697.

Furutani, Y., Y. Sudo, N. Kamo, and H. Kandori. 2003. FTIR spectroscopy of the complex between *pharaonis* phoborhodopsin and its transducer protein. *Biochemistry.* 42:4837–4842.

Gordeliy, V. I., J. Labahn, R. Moukhametzianov, R. Efremov, J. Granzin, R. Schlesinger, G. Buldt, T. Savopol, A. J. Scheidig, J. P. Klare, and M. Engelhard. 2002. Molecular basis of transmembrane signaling by sensory rhodopsin II-transducer complex. *Nature.* 419:484–487.

Grigorieff, N. T., A. Ceska, K. H. Downing, J. M. Baldwin, and R. Henderson. 1996. Electron crystallographic refinement of the structure of bacteriorhodopsin. *J. Mol. Biol.* 259:393–421.

Hirayama, J., Y. Iwamoto, Y. Shichida, N. Kamo, H. Tomioka, and T. Yoshizawa. 1992. A photocycle of phoborhodopsin from haloalkaliphilic bacterium (*Natronobacterium pharaonis*) studied by low-temperature spectroscopy. *Biochemistry.* 31:2093–2098.

Hoff, W. D., K.-H. Jung, and J. L. Spudich. 1997. Molecular mechanism of photosignaling by archaeal sensory rhodopsins. *Annu. Rev. Biophys. Biomol. Struct.* 26:223–258.

Hohenfeld, I. P., A. Ansgar, A. Wegener, and M. Engelhard. 1999. Purification of histidine tagged bacteriorhodopsin, *pharaonis* sensory rhodopsin II functionally expressed in *Escherichia coli.* *FEBS Lett.* 442:198–202.

Kamhira, M., A. Naito, K. Nishimura, S. Tuzi, and H. Saitô. 1998. A high-resolution solid-state ^{13}C and ^{15}N NMR study on crystalline Leu- and Met-enkephalins: distinction of polymorphs, backbone dynamics and local conformational rearrangements induced by dehydration or freezing motions of bound solvent molecules. *J. Phys. Chem. B.* 102:2826–2834.

Kamo, N., K. Shimono, M. Iwamoto, and Y. Sudo. 2001. Photochemistry and photoinduced proton-transfer by *pharaonis* phoborhodopsin. *Biochemistry (Moscow)*. 66:1277–1282.

Kandori, H., K. Shimono, Y. Sudo, M. Iwamoto, Y. Shichida, and N. Kamo. 2001. Structural changes of *pharaonis* phoborhodopsin upon photoisomerization of the retinal chromophore: infrared spectral comparison with bacteriorhodopsin. *Biochemistry.* 40:9238–9246.

Kawase, Y., M. Tanio, A. Kira, S. Yamaguchi, S. Tuzi, A. Naito, M. Kataoka, J. K. Lanyi, R. Needleman, and H. Saitô. 2000. Alteration of conformation and dynamics of bacteriorhodopsin induced by protonation of Asp[85] and deprotonation of Schiff base as studied by ^{13}C NMR. *Biochemistry.* 39:14472–14480.

Kim, S.-H., and K. K. Kim. 2002. Dynamic and clustering model of bacterial chemotaxis receptors: structural basis for signaling and high sensitivity. *Proc. Natl. Acad. Sci. USA.* 99:11611–11615.

Kimura, S., A. Naito, S. Tuzi, and H. Saitô. 2001. A ^{13}C NMR study on [3-^{13}C]-, [1-^{13}C]Ala-, or [1-^{13}C]Val-labeled transmembrane peptides of bacteriorhodopsin in lipid bilayers: insertion, rigid-body motions, and local conformational fluctuations at ambient temperature. *Biopolymers.* 58:78–88.

Krimm, S., and A. M. Dwivedi. 1982. Infrared spectrum of the purple membrane: clue to a proton conduction mechanism? *Science.* 216: 407–408.

Kunji, E. R., E. N. Spudich, R. Grissharmer, R. Henderson, and J. L. Spudich. 2001. Electron crystallographic analysis of two-dimensional crystals of sensory rhodopsin II: a 6.9 Å projection structure. *J. Mol. Biol.* 308:279–293.

Lanyi, J. K. 1999. Understanding structure in the light-driven proton pump bacteriorhodopsin. *J. Struct. Biol.* 124:164–178.

Le Moual, H., and D. E. Koshland, Jr. 1996. Molecular revolution of the C-terminal cytoplasmic domain of a superfamily of bacterial receptors involved in taxis. *J. Mol. Biol.* 261:568–585.

Levit, M. N., T. W. Grebe, and J. B. Stock. 2002. Organization of the receptor-kinase signaling array that regulates *Escherichia coli* chemotaxis. *J. Biol. Chem.* 277:36748–36754.

Luecke, H., B. Schobert, J. K. Lanyi, E. N. Spudich, and J. L. Spudich. 2001. Crystal structure of sensory rhodopsin II at 2.4 Ångstroms: insight into color tuning and transducer interaction. *Science.* 293: 1499–1503.

Luecke, H., B. Schobert, H.-T. Richter. J. P. Cartailler, and J. K. Lanyi. 1999. Structure of bacteriothodopsin at 1.55 Å resolution. *J. Mol. Biol.* 291:899–911.

Lybarger, S. R., and J. R. Maddock. 2000. Differences in the polar clustering of the high- and low-abundance chemoreceptors of *Escherichia coli*. *Proc. Natl. Acad. Sci. USA*. 97:8057–8062.

Rothwell, W. T., and J. S. Waugh. 1981. Transverse relaxation of dipolar coupled spin systems under RF irradiation. *J. Chem. Phys.* 75:2721–2732.

Royant, A., P. Nollert, K. Edman, R. Neutze, E. M. Landau, E. Pebay-Peyroula, and J. Navarro. 2001. X-ray structure of sensory rhodopsin II at 2.1-Å resolution. *Proc. Natl. Acad. Sci. USA*. 98:10131–10136.

Saitô, H. 1986. Conformation-dependent ^{13}C chemical shifts: a new means of conformational characterization as obtained by high-resolution solid-state NMR. *Magn. Reson. Chem.* 24:835–852.

Saitô, H., and I. Ando. 1989. High-resolution solid-state NMR studies of synthetic and biological macromolecules. *Annu. Rev. NMR Spectrosc.* 21:209–290.

Saitô, H., J. Mikami, S. Yamaguchi, M. Tanio, A. Kira, T. Arakawa, K. Yamamoto, and S. Tuzi. 2004. Site-directed ^{13}C solid-state NMR studies on membrane proteins: strategy and goals toward revealing conformation and dynamics as illustrated for bacteriorhodopsin labeled with [1-^{13}C]amino-acid residues. *Magn. Reson. Chem.* 42:218–230.

Saitô, H., T. Tuchida, K. Ogawa, T. Arakawa, S. Yamaguchi, and S. Tuzi. 2002b. Residue-specific millisecond to microsecond fluctuations in bacteriorhodopsin induced by disrupted or disorganized two-dimensional crystalline lattice, through modified lipid-helix and helix-helix interactions, as revealed by ^{13}C NMR. *Biochim. Biophys. Acta.* 1565:97–106.

Saitô, H., S. Tuzi, and A. Naito. 1998. Empirical versus nonempirical evaluation of secondary structure of fibrous and membrane proteins by solid-state NMR: a practical approach. *Annu. Rev. NMR Spectrosc.* 36:79–121.

Saitô, H., S. Tuzi, M. Tanio, and A. Naito. 2002a. Dynamic aspects of membrane proteins and membrane associated peptides as revealed by ^{13}C NMR: lessons from bacteriorhodopsin as an intact protein. *Annu. Rev. NMR Spectrosc.* 47:39–108.

Saitô, H., S. Tuzi, S. Yamaguchi, M. Tanio, and A. Naito. 2000. Conformation and dynamics of bacteriorhodopsin revealed by ^{13}C NMR. *Biochim. Biophys. Acta.* 1460:39–48.

Saitô, H., K. Yamamoto, S. Tuzi, and S. Yamaguchi. 2003. Backbone dynamics of membrane proteins in lipid bilayers: the effect of two-dimensional array formation as revealed by site-directed solid-state ^{13}C NMR studies on [3-^{13}C]Ala- and [1-^{13}C]Val-labeled bacteriorhodopsin. *Biochim. Biophys. Acta.* 1616:127–136.

Saitô, H., and M. Yokoi. 1992. A ^{13}C NMR study on collagens in the solid state: hydration/dehydration-induced conformational change of collagen and detection of internal motions. *J. Biochem. (Tokyo).* 111:376–382.

Seidel, R., B. Scharf, M. Gautel, K. Kleine, D. Oesterhelt, and M. Engelhard. 1995. The primary structure of sensory rhodopsin II: a member of an additional retinal protein subgroup is coexpressed with its transducer, the halobacterial transducer of rhodopsin II. *Proc. Natl. Acad. Sci. USA.* 92:3036–3040.

Shimono, K., M. Iwamoto, M. Sumi, and N. Kamo. 1997. Functional expression of *pharaonis* phoborhodopsin in *Escherichia coli*. *FEBS Lett.* 420:54–56.

Spudich, J. L., C. S. Yang, K. H. Jung, and E. N. Spudich. 2000. Retinylidene proteins: structures and functions from archaea to humans. *Annu. Rev. Cell Dev. Biol.* 16:365–392.

Sudo, Y., M. Iwamoto, K. Shimono, and N. Kamo. 2001b. *Pharaonis* phoborhodopsin binds to its cognate truncated transducer even in the presence of a detergent with a 1:1 stoichiometry. *Photochem. Photobiol.* 74:489–494.

Sudo, Y., M. Iwamoto, K. Shimono, and N. Kamo. 2002. Association of *pharaonis* phoborhodopsin with its cognate transducer decreases the photo-dependent reactivity by water-soluble reagents of azide and hydroxylamine. *Biochim. Biophys. Acta.* 1558:63–69.

Sudo, Y., M. Iwamoto, K. Shimono, M. Sumi, and N. Kamo. 2001a. Photo-induced proton transport of *pharaonis* phoborhodopsin (sensory rhodopsin II) is ceased by association with the transducer. *Biophys. J.* 80:916–922.

Suwelack, D., W. P. Rothwell, and J. S. Waugh. 1980. Slow molecular motion detected in the NMR spectra of rotating solids. *J. Chem. Phys.* 73:2559–2569.

Takahashi, T., H. Tomioka, N. Kamo, and Y. Kobatake. 1985. A photosystem other than PS370 also mediates the negative phototaxis of *Halobacterium halobium*. *FEMS Microbiol. Lett.* 28:161–164.

Tomioka, H., T. Takahashi, N. Kamo, and Y. Kobatake. 1986. Flash spectrophotometric identification of a fourth rhodopsin-like pigment in *Halobacterium halobium*. *Biochem. Biophys. Res. Commun.* 139:389–395.

Tuzi, S., A. Naito, and H. Saitô. 1994. ^{13}C NMR study on conformation and dynamics of the transmembrane α-helices, loops, and C-terminus of [3-^{13}C]Ala-labeled bacteriorhodopsin. *Biochemistry.* 33:15046–15052.

Umemura, T., Y. Matsumoto, K. Ohnishi, M. Homma, and I. Kawagishi. 2002. Sensing of cytoplasmic pH by bacterial chemoreceptors involves the linker region that connects the membrane-spanning and the signal-modulating helices. *J. Biol. Chem.* 277:1583–1598.

Wegener, A.-A., I. Chizhov, M. Engelhard, and H.-J. Steinhoff. 2000. Time-resolved detection of transient movement of helix F in spin-labelled *pharaonis* sensory rhodopsin II. *J. Mol. Biol.* 301:881–891.

Wegener, A.-A., J. P. Klare, M. Engelhard, and H.-J. Steinhoff. 2001. Structural insight into the early steps of receptor-transducer signal transfer in archaeal phototaxis. *EMBO J.* 20:5312–5319.

Yamaguchi, S., S. Tuzi, T. Seki, M. Tanio, R. Needleman, J. K. Lanyi, A. Naito, and H. Saitô. 1998. Stability of the C-terminal α-helical domain of bacteriorhodopsin that protruded from the membrane surface, as studied by high-resolution solid-state ^{13}C NMR. *J. Biochem. (Tokyo).* 123:78–86.

Yamaguchi, S., S. Tuzi, M. Tanio, A. Naito, J. K. Lanyi, R. Needleman, and H. Saitô. 2000. Irreversible conformational change of bacteriorhodopsin induced by binding of retinal during its reconstitution to bacteriorhodopsin, as studied by ^{13}C NMR. *J. Biochem. (Tokyo).* 127:861–869.

Yamaguchi, S., S. Tuzi, K. Yonebayashi, A. Naito, R. Needleman, J. K. Lanyi, and H. Saitô. 2001. Surface dynamics of bacteriorhodopsin as revealed by ^{13}C NMR studies on [^{13}C]Ala-labeled proteins: detection of millisecond or microsecond motions in interhelical loops and C-terminal α-helix. *J. Biochem. (Tokyo).* 129:373–382.

Yang, C. S., and J. L. Spudich. 2001. Light-induced structural changes occur in the transmembrane helices of the *Natronobacterium pharaonis* HtrII transducer. *Biochemistry.* 98:13655–13659.

Yonebayashi, K., S. Yamaguchi, S. Tuzi, and H. Saitô. 2002. Cytoplasmic surface structures of bacteriorhodopsin modified by site-directed mutations and cation binding as revealed by ^{13}C NMR. *Eur. Biophys. J.* 32:1–11.

Zhang, X.-N., J. Zhu, and J. L. Spudich. 1999. The specificity of interaction of archaeal transducers with their cognate sensory rhodopsins is determined by their transmembrane helices. *Proc. Natl. Acad. Sci. USA.* 96:857–862.